Radiocarbon Chronology/Growth Rates of Ooids from Great Salt Lake, Utah

Olivia P. Paradis[1], Frank A. Corsetti[1], Audra Bardsley[2], Douglas E. Hammond[1], William Berelson[1], Xiaomei Xu[3], Jennifer Walker[3], and Aaron Celestian[4]

[1]*Department of Earth Sciences, University of Southern California, Los Angeles, Calirforia; opiazza@usc.edu*
[2]*Environmental Studies Program, University of Southern California, Los Angeles, California*
[3]*Department of Earth System Science, University of California, Irvine, California*
[4]*Department of Mineral Sciences, Natural History Museum of Los Angeles County, Los Angeles, California*

10.31711/ugap.v51i.137

ABSTRACT

Ooids (calcium carbonate coated grains) are common in carbonate environments throughout geologic time, but the mechanism by which they form remains unclear. In particular, the rate of ooid growth remains elusive in all but a few modern marine environments. In order to investigate the rate of ooid growth in a non-marine setting, we used ^{14}C to date ooids from Great Salt Lake, Utah, a well-known site of aragonitic ooids. Bulk ooids obtained from the northern shore of Antelope Island and the northeast shore of Great Salt Lake near Spiral Jetty were sieved into different size fractions and produced mean ages ranging between 2728±15 and 4373±20 ^{14}C yr BP. Larger ooids were older than smaller ooids, implying that larger ooids grew in the environment for a longer duration, with the caveat that bulk age dating integrates the growth history of an ooid. To better resolve growth history, ooids from the coarse fraction were sequentially dissolved, and ^{14}C ages were obtained for each dissolution step to create a time series of ooid growth. The results of the sequential dating indicate that the coarse Great Salt Lake ooid growth began between 5800-6600 ± 60 ^{14}C yr BP while their outer cortices are nearly modern. Sequentially dated ooids from the South Arm of Great Salt Lake at Antelope Island record a nearly linear growth history (~ 10-15 μm/kyr), whereas ooids from Spiral Jetty record somewhat faster growth between ~6000 and 4000 years ago (0.03 – 0.06 μm/yr) followed by a 10x slower growth history for the remainder of their lifespan (0.003 – 0.008 μm/yr). The lifespan of Great Salt Lake aragonitic ooids is two to six times longer than those from modern marine environments, and thus provides a unique end member for understanding the mechanisms behind ooid formation. The ooid age range indicates that geochemical parameters measured from bulk ooid dissolution integrates over ~6000 years and thus does not represent a geochemical snapshot in time, as some previous studies have suggested.

INTRODUCTION

Ooids are small (generally <2 mm) laminated, coated grains, with a calcium carbonate cortex surrounding a nucleus. Ooids are ubiquitous in the geologic record in marine and lacustrine settings, and as accretionary structures, may serve as repositories of high resolution aqueous evolution, preserving both biogeochemical (Diaz and others, 2015, 2013; Summons and others, 2013) and isotopic (Duguid and others, 2010) information. Despite their ubiquity, ooid formation remains enigmatic. Both abiogenic and biogenic modes of formation have been proposed (Diaz and others, 2013, 2015, 2017; O'Reilly and others, 2017; Pacton and others, 2012; Summons and others, 2013), and the rate of ooid accretion remains elusive for the majority of ooid occurrences. Without a better understanding of how rapidly ooids form, their utility as paleoenvironmental indicators is hindered and the question of biogenicity remains unclear.

Radiocarbon (^{14}C; half-life = 5730 ± 40 yr) has been successfully used for the step-wise dating of marine ooids from the Bahamas (Beaupré and others, 2015; Duguid and others, 2010), Australia (Beaupré and others, 2015; James and others, 2004), and Hawaii (Hearty and others, 2010). Regardless of location, ^{14}C ages decrease from the ooid nuclei toward their outer surfaces with the exception of a ^{14}C anomaly of unknown origin in ooids from Highborne Cay, Bahamas (Beaupré and others, 2015). Using the radiocarbon chronology, Beaupré and others (2015) argued "modern" marine ooid net growth rates were slow and relatively constant, with mean lifespans ranging from 800 ± 135 to 1470 ± 280 ^{14}C years and growth rates ranging from 0.36 ± 0.03 to 2.2 ± 0.3 ng C-$CaCO_3$/ooid-year. However, calculated net growth rates from these radiocarbon dating experiments on ooids are likely underestimating gross carbonate precipitation due to abrasion, as lab experiments have shown growth can be four orders of magnitude faster than radiocarbon net growth rates (Trower and others, 2017).

The Great Salt Lake (GSL) in Utah provides a

unique opportunity to assess the net growth rate of radial aragonitic ooids that texturally resemble many ancient ooids, both marine and lacustrine (Figure 1). In addition to their utility in understanding radial ooid formation, GSL ooids may be targets for understanding the history of GSL, which as a terminal lake with no outflow, is particularly sensitive to climatic shifts. The GSL has also been subjected to environmental alteration by human activity. Especially notable is the partitioning of the lake by a railroad causeway constructed in 1959, which created a northern and southern salinity contrast. However, like marine ooids, the utility of lacustrine ooids in reconstructing paleoenvironmental changes is dependent on their placement within a proper temporal framework. The aim of this study is to use ^{14}C as a chronometer to sequentially date ooids from Great Salt Lake, and thus constrain modern ooid formation in this setting and provide necessary chronological context so that their potential as paleoenvironmental indicators may be explored.

Great Salt Lake

Great Salt Lake Environmental Setting

Great Salt Lake (GSL) is a terminal lake in northern Utah with circumneutral pH. GSL represents the present phase (since 11.5 ka BP) that resulted from

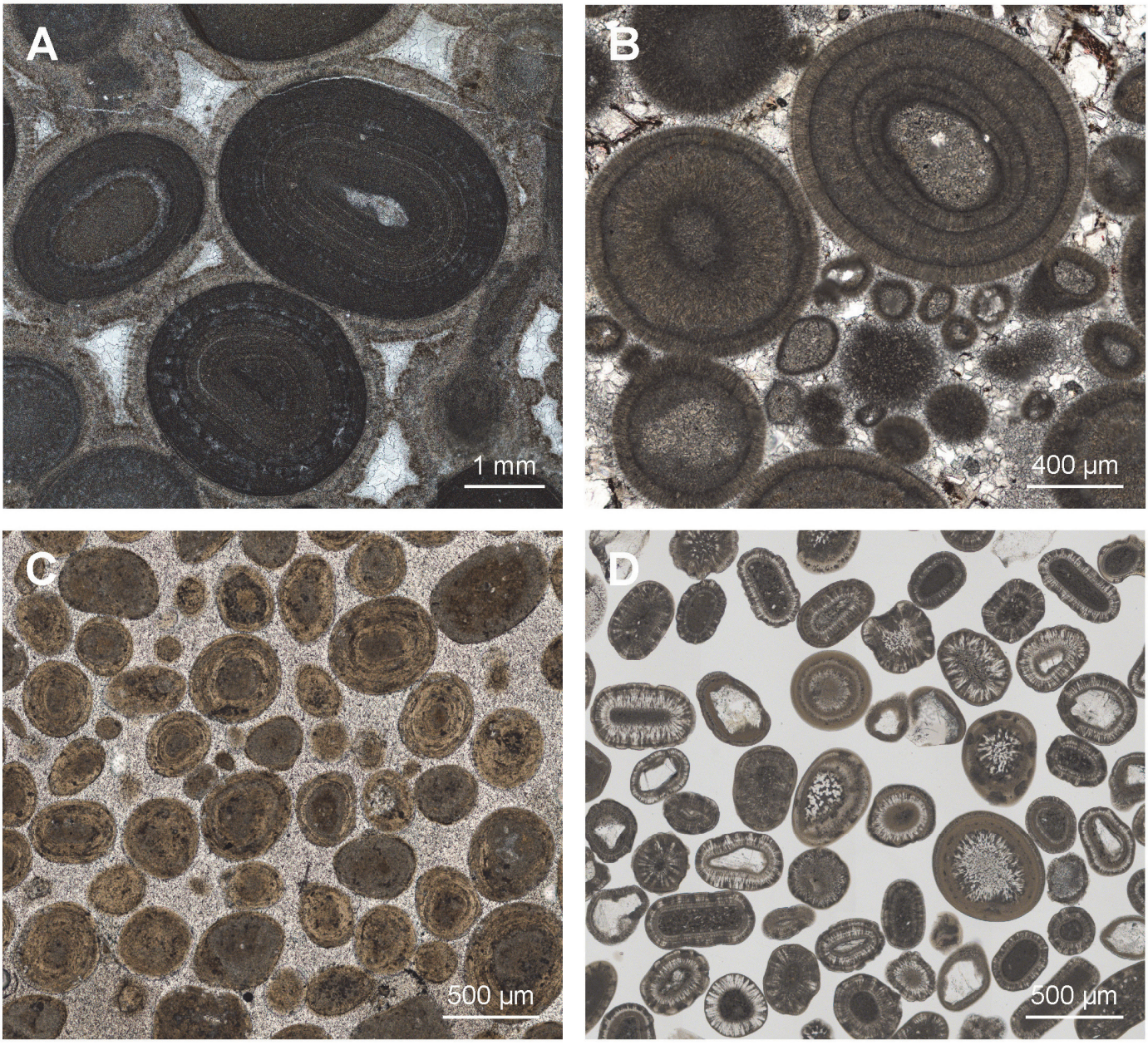

Figure 1. *Examples of ancient and modern ooid microfabrics. A) Neoproterozoic tangential ooids from the Beck Springs formation. B) Radial ooids from the Neoproterozoic Johnnie formation. C) Modern ooids from Joulter's Cay, Bahamas display tangential concentric laminae that are characteristic of many modern marine ooids. D) Modern ooids from Great Salt Lake, Utah have a primary radial crystal orientation.*

the transition of the larger and deeper Lake Bonneville (30-11.5 ka BP) to a shallow, hypersaline lake (Oviatt and others, 1992; Oviatt and others, 2015). The Holocene shallow lake interval of Great Salt Lake is accompanied by a shift to aragonite precipitation, which is in agreement with the Mg^{2+}/Ca^{2+} ratios of the lake water (Spencer 1985). The north arm of GSL is currently separated from the south arm by a rock-fill railroad causeway that was constructed in 1959. Because the three rivers that feed the lake (Bear, Jordan, and Weber rivers) enter the south arm, the north arm water is more saline (28%, at or above saturation for halite) than the south arm, which has a salinity of approximately 15% (Rupke and Macdonald, 2012; Stephens, 1990; USGS, 2023). The causeway was breached in 2016 to restore the flow between the north and south arms, but the berm in the bottom of the breach was raised by 4 feet in July 2022 help reduce north-to-south water flow but still allow water to flow from south to north. (Utah DNR, 2022).

Great Salt Lake Ooids

Ooids are found as shoreline deposits around the entirety of GSL (Baskin, 2014; Eardley, 1938). Eardley (1938) described the predominantly radial texture of the GSL ooid cortices, inferred ooid cortices were calcitic, and suggested that their radial texture was the result of recrystallization. The assumption of calcitic mineralogy in GSL ooids prevailed until Kahle (1974) demonstrated that GSL ooids are in fact aragonite and their cortical fabric is depositional. However, Kahle (1974) concluded aragonite-aragonite inversion had taken place. Sandberg (1975) confirmed the aragonitic mineralogy of GSL ooids, demonstrated that the radial aragonite fabric is depositional, and found no evidence that aragonite-aragonite inversion had taken place. Subsequently, Reitner (1999) suggested that organic matrices on the surface of GSL ooids could be important in the mineralization of the aragonite, and Lincoln et al. (2022) implicated sulfate reducing bacteria in the precipitation of Mg-silicates associated with some GSL ooids, and hypothesized some of the aragonite could be secondary vs. primary. Trower and others (2020) developed an approach to understand the unique cortical history of Great Salt Lake ooids, noting that the grains within the same deposit likely record similar histories, but found differences between populations of ooids across various localities in GSL. With respect to the age of the GSL ooids, (Mcguire, 2014) attempted serial dissolution of unsorted ooids from 15 cm water depth in the modern south arm of GSL that resulted in ^{14}C ages from 2024±36 yr BP (outermost composite sample) to 8144±29 yr BP (innermost composite sample), indicating that the ooids were quite old relative to modern marine examples, but the coarse sampling resolution could not discern whether modern precipitation took place. As part of a large-scale survey of the tufa-like carbonate mounds that many refer to as "microbialites", Bouton and others (2016) measured the bulk ^{14}C age of unsorted GSL ooids from the shoreline of the south arm of the lake. Their results yielded a composite ooid ^{14}C age of 3300 yr BP. Thus, while some constraints regarding the age of the ooids exist, many questions remain.

METHODS

Sample Collection

Ooids were collected at the sediment-water interface in less than 10 cm water depth from Bridger Bay on Antelope Island and near Spiral Jetty in March 2014 (Figure 2). Samples were rinsed with deionized water, dried in an oven at 50°C, and sieved to partition the ooids into discrete size fractions (125-250 µm, 250-355 µm, 355-500 µm). Ooid masses from each size fraction were normalized by mass to establish a grain size distribution (Figure 3). Unfiltered lake water was sampled from the shore of the northern tip of Antelope Island in the south arm of GSL and the beach at Spiral Jetty in the north arm of GSL in September 2016 for dissolved inorganic carbon ^{14}C analysis. Unfiltered river and well water were sampled in May 2017 from Bear, Jordan, and Weber rivers as well as a well in Ogden, Utah (Weber State University). At each site, one liter of water was collected in 1000ml size glass bottles (Fisher #06-414-8) which had been previously rinsed three times with deionized water, soaked in 10% HCl, and rinsed three more times with deionized water. The bottles were field rinsed three times before water was sampled with no head space and immediately poisoned with 100 µl of saturated $HgCl_2$ in the field to preclude later biologic activity.

Raman Spectroscopy

Raman spectra of GSL ooids were obtained using a Horiba XploRa+ micro-Raman spectrometer. Specimens were measured using an incident wavelength of 532 nm, laser slits of 200 µm, 1800 gr/mm diffraction grating, a 100x (0.9 NA) objective. Laser spot size was approximately 2 micrometers in diameter, and the laser power measured at the sample was approximately 87 (+/- 3) µW. Data were collected on individual grain mount ooids that were polished and thin-sectioned. Hyperspectral mapping was collected with

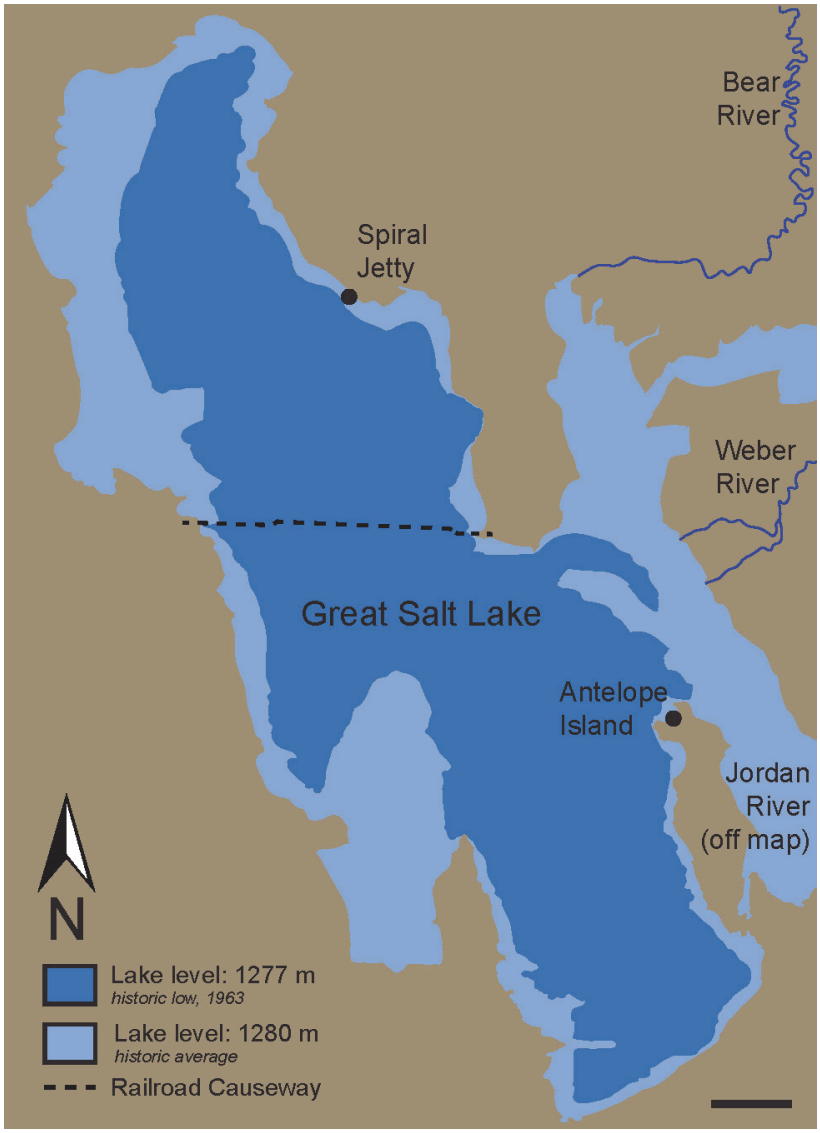

Figure 2. *Map of Great Salt Lake, modified from Currey and others, 1984. Ooid samples were collected from the sediment water interface from: Spiral Jetty in the north arm of GSL, and Bridger Bay on Antelope Island in the south arm of GSL. Scale bar equals 8km.*

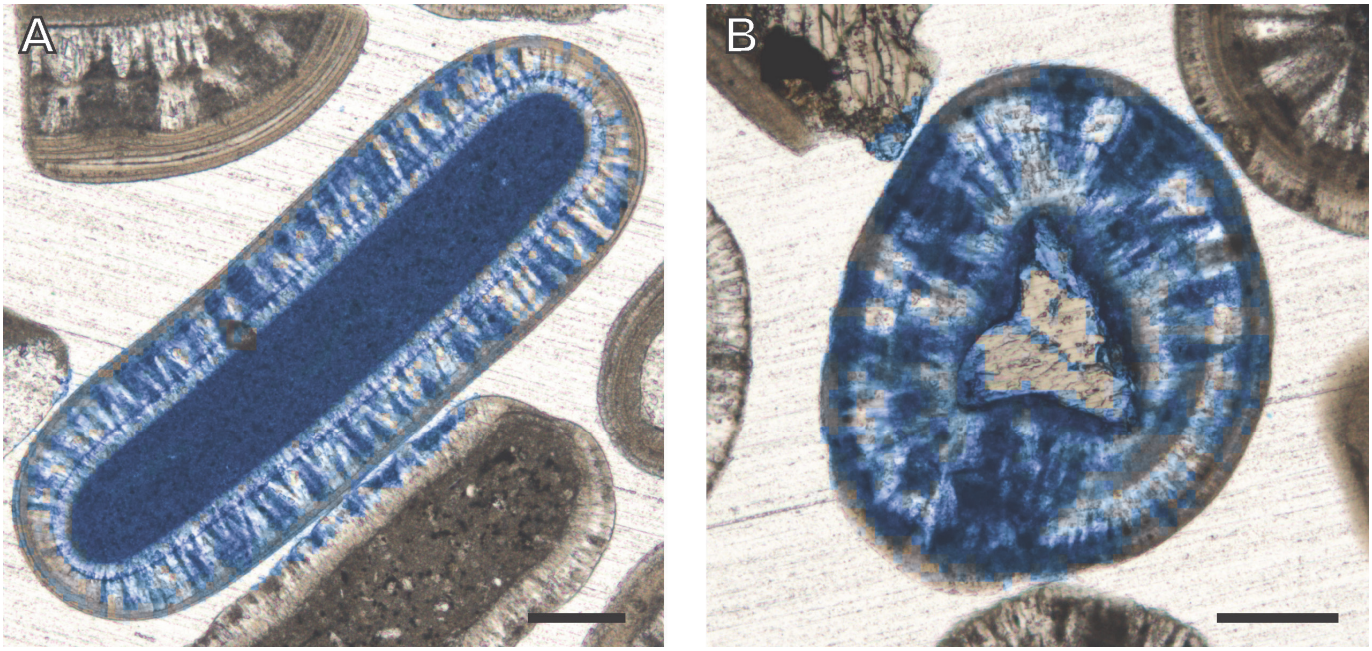

Figure 3. *Presence of organic matter (blue) within an ooid from the north arm (A) and south arm (B) of Great Salt Lake acquired from Raman spectroscopy. Only the central grain was scanned in each image. A survey of 30 ooids was carried out to confirm the distribution of organic matter within ooid cortices (SI Table 2). Scale bars equal 100 µm. Organic matter is distributed within peloidal nucleus (A) and throughout carbonate cortex (A and B).*

0.1-sec exposure averaged over three acquisitions using an 8 µm x 8 µm mapping grid. These spectral acquisition parameters were determined by trial and error to maximize signal-to-noise and keep acquisition time to less than 24 hours for most maps. After collecting hyperspectral maps, principal component analysis was performed to find those unique spectra representing the total variability within each ooid. The total number of components found for all ooids was aragonite, organic material, burned organic material (burned by the laser), pigment (carotenoid), quartz, K -feldspar, and epoxy (SI Figure 1). Microplastics were found but were exceedingly rare within the ooids. Once components were identified for each ooid, heat maps were generated by least squares fitting to every spectrum in the map (in some cases, these were >80,000 spectra per map). The least squares fitting does provide an approximate percentage of each component in the spectra; however, these values often have very high errors. Therefore, the heat maps were treated as the presence or absence of each component and were not used for absolute abundances.

Massive organic material has a characteristic Raman signal and strong luminescence with the 532 nm laser. These patterns were compared to known organic materials from pigmented crustacea after digestion by red-ear slider turtles (Clause 2021). The result is intense luminescence from the organic-rich parts of the sample, and therefore no individual organic molecule could be identified except for the carotenoids. The carotenoids were all found in spectra with organic luminescence. Attempts to collect data with a 785 nm laser resulted in very poor signal-to-noise ratio, and it was determined that large maps could not be collected in a reasonable time frame (< 24 hrs), even though the background luminescence intensity was lower. Burned organic material has characteristic D and G bands common for soot, char, and organic materials with high thermal maturity.

Dissolved Inorganic Carbon ^{14}C Age

Lake, river, and well water samples were prepared using the headspace-extraction method (Gao and others, 2014). All radiocarbon results have been corrected for isotopic fractionation according to the conventions of Stuiver and Polach (1977), with $\delta^{13}C$ values measured on prepared graphite using the AMS spectrometer. These may differ from $\delta^{13}C$ of the original material, if fractionation occurred during sample graphitization of the AMS measurement, and thus, the d13C values reported herein were measured on water dissolved inorganic carbon (DIC) directly using Gas Bench coupled with IRMS (Finnigan Delta Plus).

Bulk Inorganic and Organic Carbon Ooid ^{14}C Ages

Total organic and inorganic C was extracted from each sieved ooid sample (125-250 µm, 250-355 µm, 355-500 µm) and an unsorted ooid sample. The extracted organic and inorganic carbon was analyzed for ^{14}C at the Keck Carbon Cycle Accelerator Mass Spectrometer (KCCAMS) facility at the University of California, Irvine (Beverly and others, 2010; Southon and others, 2004). Details regarding methodology for the bulk organic and inorganic carbon extractions may be found in the supplementary information (SI Table 1).

Sequential Ooid Acidification

To assemble an ooid chronology, we measured the ^{14}C ages of fractions of CO_2 collected during sequential acid addition to sieved ooids (355-500 µm) from Spiral Jetty and Antelope Island. Ooids (~50g) and 150ml of deionized water (DIW) were placed in a reaction vessel constructed from a 500ml graduated round media storage bottle (VWR cat. # 89000-238) and a suspended magnetic stir rod (SI, Figure 2). The reaction vessel was purged with N_2 that was scrubbed with Ascarite-II while a stir bar spun at 700 rpm to drive off any dissolved CO_2 in the water for a total of 30 minutes. The sample was acidified by injecting 60 ml of 3.3M HCl at a flow rate (acid) of 10ml/min. Gas was shunted for the first 5 seconds of acidification to off-gas any residual N_2 before collecting the sample in Tedlar bags which had been rinsed with ultra-high purity (UHP) helium scrubbed with Ascarite-II. Gas was collected in 3 Tedlar bags per each acidi-

Table 1. *14C and δ13C composition of Weber, Bear, and Jordan rivers as well as well water sampled in Ogden, Utah. Dissolved inorganic carbon (DIC) is reported in millimolar (mM). Water was treated with HgCl2.*

Water Source	Latitude	Longitude	$\delta^{13}C$(‰)	±	fraction Modern	±	$\Delta^{14}C$(‰)	±	^{14}C age (yr BP)	±	DIC (mM)
Well	41.192175	-111.93894	-15.5	0.1	0.8377	0.0014	-169.1	1.4	1425	15	6.6
Weber River	41.218295	-111.987708	-10.2	0.1	0.9332	0.0015	-74.3	1.5	555	15	3.2
Bear River	41.545895	-112.095349	-8.4	0.1	0.8348	0.0016	-171.9	1.6	1450	20	4.1
Jordan River	40.771568	-111.975878	-9.7	0.1	0.8416	0.0014	-165.2	1.4	1385	15	4.1

fication step. The first Tedlar bag collected gas for the first 30 ml of acid added, the second Tedlar bag collected gas during the second 30 ml acid addition, while the third Tedlar bag collected remaining CO_2 that evolved after all 60 ml acid had been added and was left to sit for 3 minutes before pulling it off the vessel. Four discrete acidification steps were performed, with a subsample of 5-10 ooids removed from the acidification vessel between each. The subsample of ooids was examined using a Hitachi TM-1000 environmental scanning electron microscope (SEM) to confirm dissolution was occurring from the outside to the inside (SI, Figure 3). Between acidifications, ooids were rinsed three times with deionized water (DIW) and dried overnight. The reaction vessel and its components were rinsed in 10% HCl and dried between each acidification. The DIW in the reaction vessel was replaced, and the reaction vessel was purged for 30 minutes with ascarite-scrubbed N_2 to remove any atmospheric carbon. The acidification procedure, using 60 ml of 3.3 M HCl, DIW rinse, acid wash, and 30-minute purge, was repeated for each acidification (four times total). Following the final acidification, the remaining nuclei were rinsed three times with DIW, dried overnight, and reserved for ^{14}C analysis of the organic carbon fraction. Some calcium carbonate remained on the oolitic nuclei at the end of the experiment to ensure ancient carbonate nuclei were not dissolved which might skew the oldest inorganic carbon age.

^{14}C Analysis

For ^{14}C analysis, gas samples from the sequential leach were cryogenically purified through a dry ice/ethanol trap and collected in a liquid nitrogen trap. Residuals from ooid dissolution of bulk ooids and from the sequential leach were combusted at 900°C for 3 hours to obtain CO_2. All purified CO_2 samples were graphitized using a sealed-tube zinc reduction method (Xu and others, 2007). Graphite was pressed into aluminum target holders and analyzed for ^{14}C at the Keck Carbon Cycle Accelerator Mass Spectrometer (KCCAMS) facility at the University of California, Irvine (Beverly and others, 2010; Southon and others, 2004). Data were normalized to oxalic acid standard OX1 and background corrected using radiocarbon-dead reference carbonates acidified in the same reaction vessel. A modern CSTD standard (an in-house coral standard from Ellen Druffel, with a fraction modern value of 0.9445 ± 0.0018 (1σ stdev, n=262) was also processed by the acidification and measured for quality control (Gao and others, 2014). ^{14}C data are presented according to the conventions presented in Stuiver and Polach, 1977. Non-calibrated ages (given in year before present, or YBP) are presented in this paper to be consistent with ages reported in the literature.

RESULTS

^{14}C Analyses in the Great Salt Lake

The radiocarbon ages of the surface water that enters Great Salt Lake (Bear, Jordan, and Weber Rivers) and water from a groundwater well in Ogden, Utah were measured in May 2017. The ^{14}C ages of the Weber River, Bear River, and Jordan River are 555±15 yr BP, 1450±20 yr BP, and 1385±15 yr BP, respectively (Table 1). Water sampled from a groundwater well on Weber State University campus in Ogden, UT produced a ^{14}C age of 1425±15 yr BP.

Bulk Ooid ^{14}C Results

Bulk unsorted and sieved ooids from each site yield inorganic and organic ^{14}C ages that represent the average of a mix of older and younger carbon in the samples, and thus do not represent a unique age for the ooids. However, bulk ages can help bracket the general age of the ooids and provide some indication of their antiquity. In general, bulk ooid carbonate analyses produced ages that ranged from 2728±15 (Spiral Jetty) to 4373±20 yr BP (Spiral Jetty), whereas bulk organics produced slightly younger ages, between 1935±15 (Antelope Island) and 4200±15 yr BP (Spiral Jetty) (Table 2). Smaller ooids have younger average ^{14}C ages, which is reflected in both inorganic and organic carbon. Total organic carbon of bulk ooids from both sites varies from 0.43% to 1.34%; however, ooids from the north arm of GSL have more than double the organic carbon of south arm ooids (Table 2). Raman spectroscopy of ooid cross sections

Table 2. *Inorganic and organic ^{14}C ages from bulk ooids.*

Locality	Grain Size (µm)	Inorganic C Age (^{14}C yr BP)	Organic C Age (^{14}C yr BP)	% Total Organic Carbon
Spiral Jetty - North Arm				
	Unsorted	3872±15	3490±15	**1.34**
	355-500	4373±20	4200±15	1.3
	250-355	3759±15	3520±20	0.97
	125-250	2728±15	2335±15	1.19
Antelope Isl -- South Arm				
	Unsorted	3556±15	2175±20	**0.46**
	355-500	3947±15	2680±20	0.43
	250-355	3834±15	2250±15	0.48
	125-250	3158±15	1935±15	0.55

shows that organic matter is distributed both in the micritic nuclei of ooids (when the nuclei are peloids) and incorporated throughout the carbonate cortices (Figure 3, SI Figure 1). Grain size analysis reveals both north and south arm ooids are skewed toward finer grain sizes which contain more organic C in the nuclei proportionally, between 63 and 355 µm. North arm ooids are less dominated by the 63 – 355 µm size class (45%), than southern arm ooids (73%) (Figure 4).

Serial ^{14}C Ooid Record

^{14}C ages of CO_2 that was released during acidification of 355 – 500 µm diameter ooids from Spiral Jetty increased in a non-linear manner from an age of 660±15 yr BP in the first layer dissolved to 5830±60 yr BP in the last layer dissolved. The ^{14}C ages of ooids from Antelope Island increased linearly from 460±20 yr to 6600±60 yr BP (SI Table 1) (uncorrected for reservoir effect). ^{14}C ages of organic matter combusted from the nuclei remaining at the end of the experiment were 5975±15 and 6210±20 yr BP for Spiral Jetty and Antelope Island ooids, respectively.

As dissolution progresses and ooids become smaller, each successive sample taken represents a thicker width of ooid cortex dissolved (assuming the mass dissolved from each acid addition is constant), thus homogenizing the ^{14}C over a larger range of radial cortex depths. To account for this, ages were integrated over ooid cortices ranging from 355 – 500 µm in diameter assuming they had a spherical geometry and constant net growth (precipitation - abrasion) (Figure 5A, 5B) using $V = 4/3 * \pi r^3$, where V is volume and r is radius in micrometers. To summarize, our experiments indicate that 355-500 µm ooids from GSL began precipitating around 5830-6600 ± 60 ^{14}C years BP with a continuous chronology to near modern ages (when corrected for reservoir effect). Organic carbon extracted from the nuclei material left at the

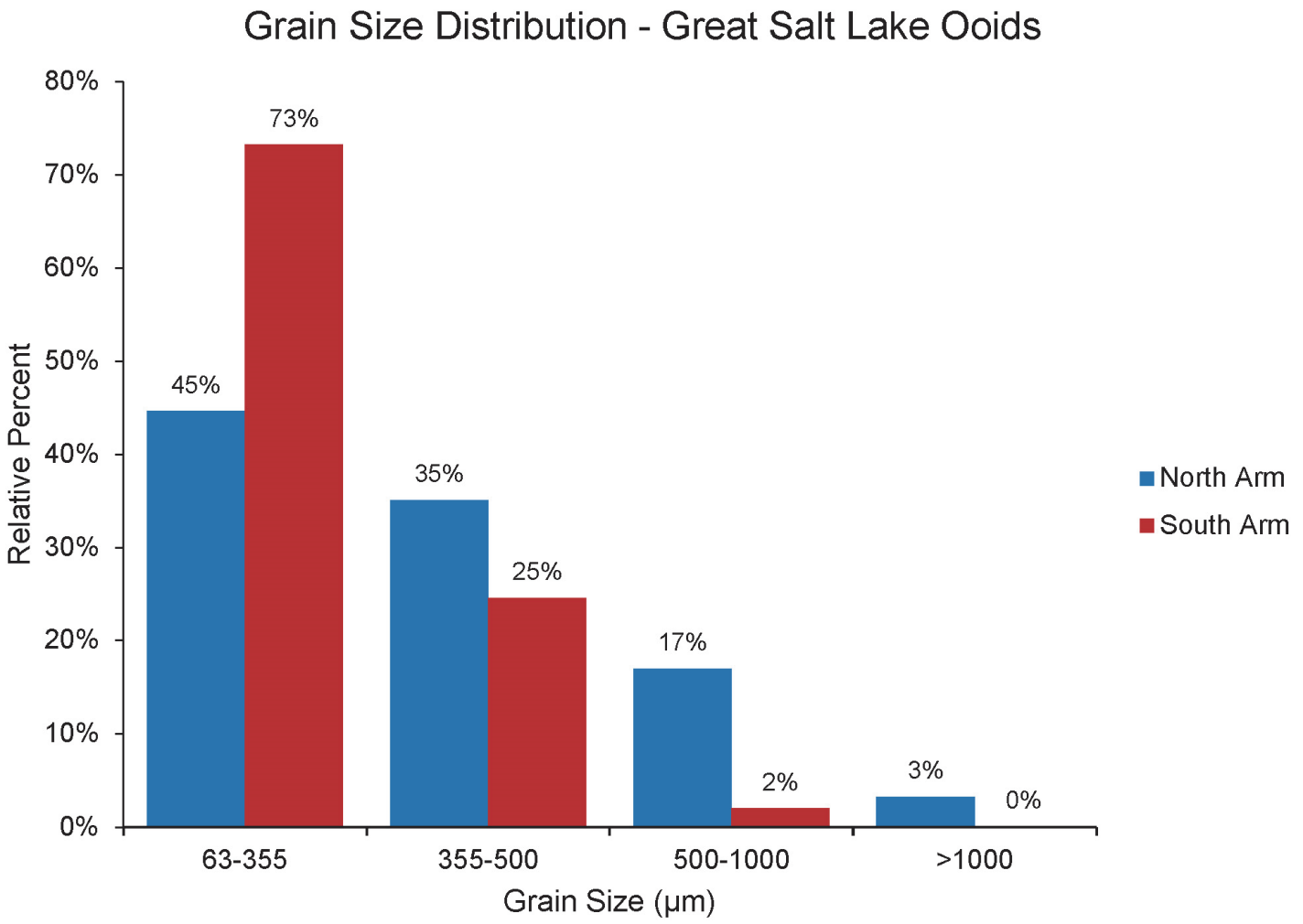

Figure 4. *Grain size distribution of Great Salt Lake ooids sampled from the north and south arms of the lake. Ooids from both arms of the lake are dominated by finer sized ooids (63 – 355 µm), though south arm ooids are more heavily skewed toward fine grain sizes.*

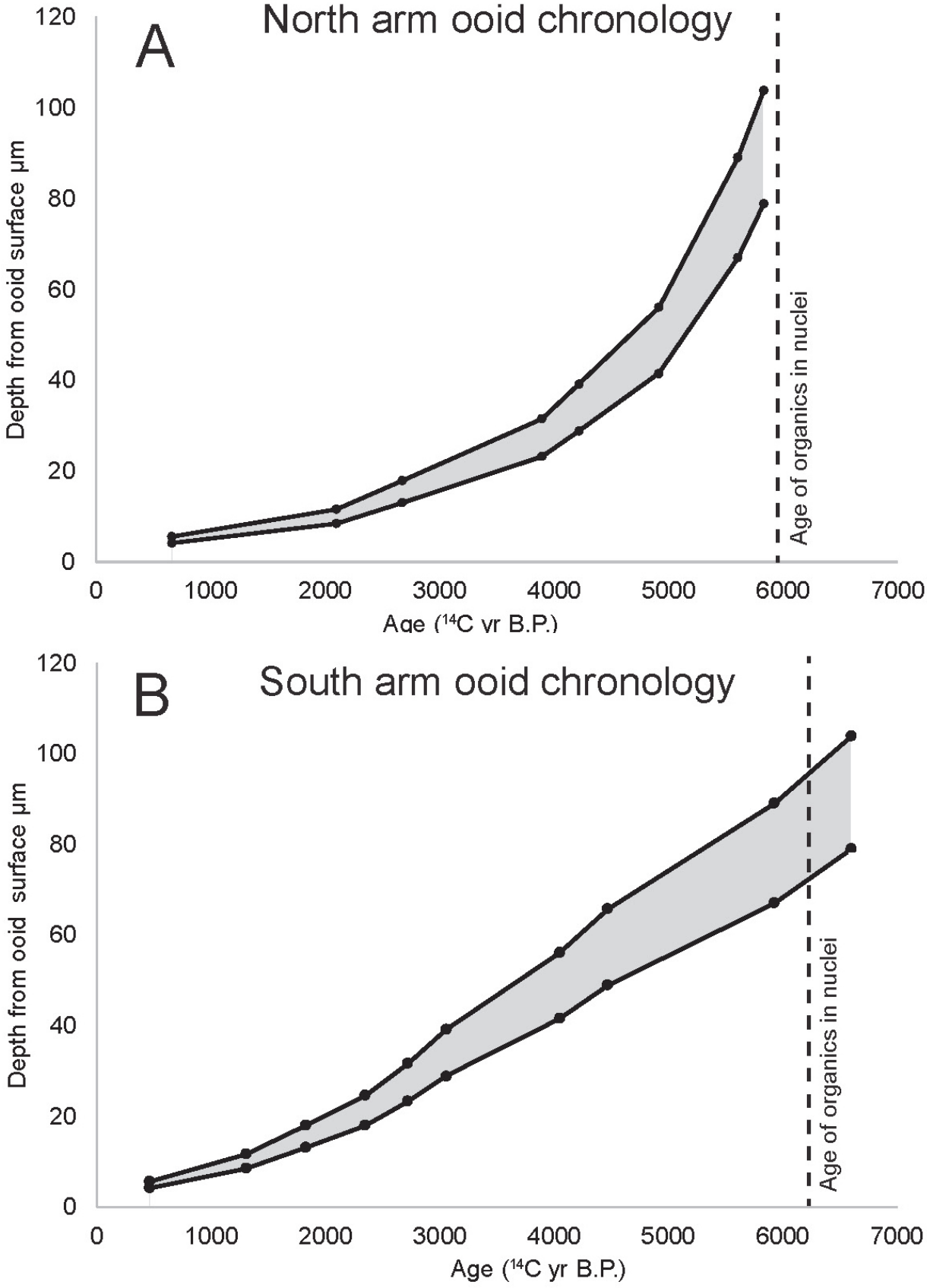

Figure 5. *Inorganic ^{14}C chronologies from north arm ooids (A) and south arm ooids (B) were integrated over ooid cortical ranges of 355-500 µm in diameter (represented by shaded region), assuming spherical geometry and constant net growth. ^{14}C ages from organic carbon (dotted line) from remaining ooid nuclei were 5975±15 and 6210±20 yr for north arm (A) and south arm (B) ooids respectively.*

end of the experiment yield nearly contemporaneous ages with the oldest inorganic carbon samples, lending credence to the presumed onset of ooid formation by our methods. The average ooid age extracted from the sequential dissolution yields mean ages of 3737 yr BP and 3277 yr BP for North and South arm ooids (355 – 500 μm diameter), respectively.

DISCUSSION

It is important to consider the behavior of ^{14}C in the GSL, as the ^{14}C age of lacustrine carbonates may be subject to a "reservoir effect", whereby lakes can accumulate old dissolved inorganic carbon over time. Lakes acquire some of this carbon from inflowing water that travels over ancient limestones that reside in their catchment, causing their dissolved inorganic carbon pool to have an apparent age that would be older than the atmospheric value. Any calcium carbonate that precipitates from that lake water would record an apparently older ^{14}C age than coeval atmospheric ^{14}C. Our analyses reveal that reservoir effects represent the largest source of uncertainty in our data. Surface water enters the lake via three rivers: Bear, Jordan, and Weber, all of which enter the south arm of GSL. Our results show that these river waters and water from a well in Ogden, Utah (representing groundwater) deliver ancient inorganic carbon to the lake. The continuous exchange of CO_2 between the lake water and the atmosphere reduces the age of the lake water reservoir, and thus the reservoir age at any given time is a reflection of the water balance of the inputs of ancient DIC, lake surface area (exchange of CO_2), DIC removal, and the existing reservoir age. Two anthropogenic changes may have influenced the lake reservoir age in contrasting ways. The causeway has reduced the north arm surface area by a factor of two, reducing the rate of atmospheric exchange in this region proportionally. However, bomb testing has increased $^{14}C/^{12}C$ in the atmosphere by an average of 50% during the past 50 years. Because those two effects may largely negate one another, we assume the modern south arm reservoir effect of 295± 20 yr BP is likely more representative of pre-causeway homogeneous lake conditions and therefore more applicable to this dataset. There remains uncertainty in how the reservoir age may have varied through the past 6000 years. Paired U-Th and ^{14}C ages from lacustrine cave carbonates suggest the reservoir effect for Lake Bonneville (from 25 to 13 ka) was 200 years or less (McGee and others, 2012), which agrees with previous estimates of Lake Bonneville's reservoir effect (Oviatt and others, 1992). However, Bowen and others (2019) suggest reservoir ages for much of the Holocene may exceed 1000 years, and they estimate that the reservoir age decreased substantially from >1200 years to <500 years during the late Holocene.

Bulk inorganic ^{14}C ages from sieved ooids reveal that smaller ooids are younger than larger ooids (Table 2). The younger average bulk ^{14}C ages of finer sized ooids may be attributed to a more recent onset in formation and implies that an ooid factory has been active in Great Salt Lake since ~6000 YBP. Therefore, ooid size in the GSL would appear to scale with age rather than some later physical sorting mechanism indicating that ooids have been growing in GSL over at least the past several thousand years at these localities. The grain size distribution is skewed toward finer grain sizes in both arms of the lake, which is also suggestive of an active ooid factory when combined with bulk ooid age data (Table 2, Figure 4). Bulk ooid ages also indicate that the Great Salt Lake ooids are significantly older than the modern marine ooids from Carbla Beach, Australia and the Bahamas (Beaupré and others, 2015; Duguid and others, 2010). However, some significant caveats require exploration while interpreting bulk ^{14}C ages. Bulk ooid ages do not allow for the differentiation between relic ooids that formed thousands of years ago versus modern ooid formation if the population of ooids in a size class is a mixture of material of different ages. In addition, Raman spectroscopy demonstrates that organic carbon is not exclusively found in peloidal nuclei but is also incorporated throughout the ooid cortex. Thus, bulk ooid organic carbon ages represent a mixture of organic carbon from *Artemia* pellet nuclei and younger organic carbon incorporated at various points in the growth of the aragonitic cortex. Ooids from the northern arm of GSL have older bulk organic carbon ages (Table 2) for each size fraction, including unsorted ooids. Because the total organic carbon content in north arm ooids is twice that of south arm ooids and the bulk organic carbon ages are older, we expect this age disparity is attributed to a higher occurrence of ooids with organic-rich brine shrimp pellet nuclei in the north arm of the lake. Petrographic investigation of 100 ooids in thin section from the northern and southern arm of GSL confirm this hypothesis, with 83% pellet nuclei in the north compared to 56% pellet nuclei in the south (SI Figure 4). The distribution of organic matter throughout ooid cortices coupled with the need to resolve a chronology from the carbonate fraction, highlight both the problems with interpreting bulk age data from ooids and the need for serial dissolution.

Our serial dissolution experiments present a chronology from modern lacustrine ooids that demonstrate the ancient onset of ooid formation over ~6,000 years ago. Once corrected for reservoir effect, the youngest inorganic carbon ages suggest ooids continued to form, apparently up to the present. We hypothesize

ooid formation may still be occurring, as any modern ^{14}C would be homogenized with slightly older ^{14}C in our youngest sample. The $^{14}C_{org}$ from Antelope Island ooids is slightly younger than the oldest inorganic carbon sample, and this may be attributed to 1) residual organics of younger origin, 2) partial leaching of ancient carbonate material in the center of the ooids, and/or 3) a reservoir effect yielding inorganic carbon which is apparently older by hundreds of years.

The age of the onset of ooid growth from the north and south arm of GSL is similar, as indicated by the oldest inorganic and organic carbon ages of ooids, but the growth curve of their chronologies varies. For example, the south arm ooids appear to have a near-constant growth rate (between ~0.01 – 0.015 μm/yr) within the resolution of the data and assumptions. In contrast, the growth of the north arm ooids appears to have been initially more rapid (~0.03 – 0.06 μm/yr) and then slowed somewhat throughout their growth history (0.003 – 0.008 μm/yr). The differences in slope (Figure 5) may be attributed to local site-specific variations affecting carbonate precipitation or abrasion in each part of the lake, or assumptions made when calculating dissolution depth (i.e., constant net growth rate, spherical geometry). To determine whether the assumption of spherical geometry in age integration is responsible for the difference in the slope of the ooid growth curves, we integrated the ages over assumed ellipsoidal ooid geometries. The resulting slope differences were exacerbated when we assumed 100% ellipsoidal geometry (SI Figure 5), suggesting that there are likely other effects (environmental, geochemical, or physical) during the ooid growth history causing their differences in slope. It is intriguing that the north arm ooids fit the prediction that ooid growth should be rapid at first and then slow as they reach hydrologic equilibrium and spend more time as bedload versus suspended load (Trower and others, 2017) but coevally, the south arm ooids display a linear growth trend. The prevailing wind direction at GSL is from the SE (Western Regional Climate Center, 2023). Because of the locations of the samples (Figure 1), the north arm site should receive stronger wave action than the south arm site, resulting in greater abrasion and slower growth as the grain grows in size. The grain size data (Fig. 4), seem to support this, as coarse grained ooids may have been selectively concentrated by stronger wave energy at the northern site.

Comparison to Marine Ooid Chronologies

The GSL ooid growth histories raise some unexpected questions with respect to how ooids form in the GSL and thus how ooids grow in general. The lifespan of 355-500 μm radial ooids from Great Salt Lake is between two and six times longer than most modern marine ooids from the Bahamas Archipelago and Australia (Beaupré and others, 2015; Duguid and others, 2010). The ooids are very old compared to modern marine examples, yet sequential dating reveals they experienced continuous net growth for over 6000 years while existing within the GSL environment. Trower and others (2017) note that the balance of precipitation versus abrasion are key components in the formation of ooids. On the one hand, the GSL has a very different chemical environment versus the marine settings. For example, in marine settings where ooids grow, the seasonal water temperature variations are low, whereas the Great Salt Lake experiences comparatively large temperature fluctuations (SI Figure 6). Paradis 2019 showed that the solubility of aragonite decreases as temperature increases and CO_2 escapes to the atmosphere, thus the favorable window for aragonite precipitation in the GSL may only exist over a short window in the summer when the lake water is significantly warmer, whereas marine settings are likely to be supersaturated with respect to aragonite year-round. Additionally, we expect abrasion is less intense in the GSL than in marine systems as GSL is a significantly lower energy environment than marine examples. Finally, the much lower Ca^{+2}/Mg^{+2} in GSL (0.03, Jones and others, 2009) compared to the ocean (0.2) may slow growth rates.

It is unclear how the balance between abrasion and precipitation should be reconciled given how slowly net ooid growth appears to be in the GSL system. Do they experience rapid growth then significant abrasion on a yearly basis, thus accounting for such a slow net growth rate, or do they simply grow very slowly? Growth could also be episodic in response to variations in salinity driven by rainfall variations on decadal (or longer) time scales. Petrographic investigation reveals what appear to be relatively delicate aragonite crystals that we speculate would not survive intense abrasion, supporting the premise that that perhaps the GSL ooids simply grow very slowly. Furthermore, how might the radial fabric affect or indicate growth rate versus the tangential fabric in modern marine ooids? Could the low Ca^{+2}/Mg^{+2} in GSL facilitate growth at the tips of crystals extending into the solution? Interestingly, Lincoln et al. (2022) hypothesized that the large ray-like aragonite crystals common in GSL ooid cortices may represent a replacement of a precursor Mg-silicate (that is, not a primary phase, but one formed later vs. adjacent, subjacent, or superjacent aragonite). We note that the ^{14}C chronologies of all sampled ooids are coherent (inside/older-outside/younger from initiation of growth to termination for the sequentially dated ooids, with the ^{14}C organic dates of the nuclei corroborating the initiation of ooid growth, as well as larg-

older-smaller/younger for the bulk dated ooid). While our work cannot comment on the paragenetic sequence of the ooid fabrics, the coherence of ^{14}C ages is unexpected if secondary replacement of aragonite was widespread. Future work, including finer scale sequential dating, may help resolve the unanswered questions surrounding the GSL ooids.

Ooids and the History of the Great Salt Lake

During ooid growth, the north and south arms of Great Salt Lake would have been in communication with one another as part of one large body of water (rather than two arms separated by a railway), thus the generally similar chronologies for onset of ooid growth from each arm of the lake ~6000 years ago agrees with the lake's history. Furthermore, 10,000 ^{14}C yr BP marks the end of the Gilbert episode of Great Salt Lake, where the lake experienced a brief 15m transgression during which the lake had freshened enough to support ostracods and possibly fish (Broughton and others, 2000; Oviatt and others, 2015). After the Gilbert episode, GSL regressed to average historic GSL levels (near 1280 m) and brine shrimp cysts and pellets appeared in lake sediment cores (Oviatt and others, 2015). It is thought that Great Salt Lake did not transgress higher than modern lake levels during early parts of the Holocene (11.5-10.2 cal ka BP; 10-9 ^{14}C ka BP), but little is known about the remainder of Holocene lake level because Holocene sediments on the floor of GSL have been largely reworked (Oviatt and others, 2015). On one hand, a bulk chemical analysis of ooids would represent an homogenized signal over ~6000 years and provides one outlook for the duration of aquatic history that ooids may represent, with relevance to other systems where ooids are analyzed as paleoenvironmental indicators. On the other hand, sequential dissolution of the ooids preserved in GSL ooids has the potential to resolve some of the finer scale lake level variations in GSL during the last ~6,000 years and potentially longer given that $\delta^{13}C$ and $\delta^{18}O$ are coupled in this closed-basin system, and $\delta^{18}O$ can correlate with lake level (e.g., Talbot 1990).

CONCLUSIONS

The high-resolution ^{14}C chronology of GSL ooids demonstrates that: ^{14}C is a robust tool for dating ooids in GSL, and GSL ooids have a lifespan between two and six times longer than modern marine ooids. The long ooid lifespan confirms the need to temporally resolve accretionary structures like ooids before interpreting bulk geochemical data. The ^{14}C ages obtained from organics in ooid nuclei corroborate the timeframe of onset of aragonite precipitation. Additionally, Raman spectroscopy coupled with ^{14}C ages from bulk unsorted and sieved ooids shed light on the importance of sequentially derived chronologies due to the fact that bulk ages underestimate the maximum age of ooids by thousands of ^{14}C years. This study highlights the disparity in net growth rate, lifespan, and seasonality in precipitation between radial ooids from Great Salt Lake and modern marine ooids. Ooids from different parts of the lake show differing growth histories, perhaps reflecting localized variations in wave energy due to prevailing wind direction or other local environmental conditions. Lastly, the >6000 year chronology captured in GSL ooids highlights the caution needed in utilizing these accretionary sediments in a bulk geochemical analysis as ooids are repositories of thousands of years of environmental change.

ACKNOWLEDGEMENTS

We thank Bonnie Baxter and Jaimi Butler for their support in organizing field sampling. We also thank Dr. Carie Frantz, Dr. Victoria Petryshyn, Dr. Dylan Wilmeth, Dr. Scott Perl, Dr. John Spear and Dr. Joyce Yager for their helpful assistance in the field and Nick Rollins for help in the lab. This work was supported in part by the SEPM student research award.

REFERENCES

Baskin, R. 2014. *Occurrance and Spatial Distribution of Microbial Bioherms in Great Salt Lake, Utah*. University of Utah.

Beaupré, S. R., Roberts, M. L., Burton, J. R., & Summons, R. E. 2015. Rapid, high-resolution ^{14}C chronology of ooids. *Geochimica et Cosmochimica Acta*, *159*, 126–138. https://doi.org/10.1016/j.gca.2015.03.009

Beverly, R. K., Beaumont, W., Tauz, D., Kaelyn, M. O., Karl, F. V. R., Guaciara, M. S., & Southon, J. R. 2010. The Keck Carbon Cycle AMS Laboratory, University of California, Irvine: Status Report. *RADIOCARBON*, *52*, 301–309. Retrieved from https://www.ess.uci.edu/researchgrp/ams/files/beverly_et_al_2010_52_2.pdf

Bouton, A., Vennin, E., Boulle, J., Pace, A., Bourillot, R., Thomazo, C., … Visscher, P. T. 2016. Linking the distribution of microbial deposits from the Great Salt Lake (Utah, USA) to tectonic and climatic processes. *Biogeosciences*, *13*(19), 5511–5526. https://doi.org/10.5194/bg-13-5511-2016

Bouton, A., Vennin, E., Mulder, T., Pace, A., Bourillot, R., Thomazo, C., … Visscher, P. T. 2016. Enhanced development of lacustrine microbialites on gravity flow deposits, Great Salt Lake, Utah, USA. *Sedimentary Geology*, *341*, 1–12. https://doi.org/10.1016/j.sedgeo.2016.05.004

Bowen, G., Nielson, K., & Eglinton, T. 2019. Multi-Substrate Radiocarbon Data Constrain Detrital and Reservoir Effects in Holocene Sediments of the Great Salt Lake, Utah. Radiocarbon, 61(4), 905-926. doi:10.1017/RDC.2019.62

Broughton, J. M., Madsen, D. B., & Quade, J. 2000. Fish Remains from Homestead Cave and Lake Levels of the Past 13,000 Years in the Bonneville Basin. *Quaternary Research*, *53*(3), 392–401. https://doi.org/10.1006/QRES.2000.2133

Clause, A. G., Celestian, A. J., & Pauly, G. B. (2021). Plastic ingestion by freshwater turtles: a review and call to action. Scientific Reports, 11(1), 1-10.

Currey, D. R., Atwood, G., & Mabey, D. R. 1984. Major levels of Great Salt Lake and Lake Bonneville. *Utah Geological and Mineral Survey Map 73*.

Diaz, M., Eberli, G., Blackwelder, P., Phillips, B., & Swart, P. 2017. Microbially mediated organomineralization in the formation of ooids. *Geology*, *45*(9). https://doi.org/10.1130/G39159.1

Diaz, M., Piggot, A., Eberli, G., & Klaus, J. 2013. Bacterial community of oolitic carbonate sediments of the Bahamas Archipelago. *Marine Ecology Progress Series*, *485*, 9–24. https://doi.org/10.3354/meps10359

Diaz, M., Swart, P., Eberli, G., Oehlert, A., Devlin, Q., Saeid, A., & Altabet, M. 2015. Geochemical evidence of microbial activity within ooids. *Sedimentology*, *62*(7), 2090–2112. https://doi.org/10.1111/sed.12218

Duguid, S. M. A., Kyser, T. K., James, N. P., & Rankey, E. C. 2010. Microbes and Ooids. *Journal of Sedimentary Research*, *80*(3), 236–251. https://doi.org/10.2110/jsr.2010.027

Eardley, A. J. 1938. the American Association of Petroleum Geologists. *Bulletin of the American Association of Petroleum Geologists*, *22*(10), 1305–1363. https://doi.org/10.1126/science.58.1489.27

Gao, P., Xu, X., Zhou, L., Pack, M. A., Griffin, S., Santos, G. M., … Liu, K. 2014. Rapid sample preparation of dissolved inorganic carbon in natural waters using a headspace-extraction approach for radiocarbon analysis by accelerator mass spectrometry. *Limnology and Oceanography: Methods*, *12*(APR), 174–190. https://doi.org/10.4319/lom.2014.12.174

"Great Salt Lake Causeway Berm Raised 4 Feet to Protect Salinity Levels." Utah Division of Forestry, Fire & State Lands, Utah DNR, https://ffsl.utah.gov/uncategorized/dnr-modifies-great-salt-lake-causeway-breach-in-response-to-salinity-issues/.

Hearty, P. J., Webster, J. M., Clague, D. A., Kaufman, D. S., Bright, J., Southon, J., & Renema, W. 2010. A pulse of ooid formation in Maui Nui (Hawaiian Islands) during Termination I. *Marine Geology*, *268*, 152–162. https://doi.org/10.1016/j.margeo.2009.11.007

James, N. P., Bone, Y., Kyser, T. K., Dix, G. R., & Collins, L. B. 2004. The importance of changing oceanography in controlling late Quaternary carbonate sedimentation on a high-energy, tropical, oceanic ramp: north-western Australia. *Sedimentology*, *51*(6), 1179–1205. https://doi.org/10.1111/j.1365-3091.2004.00666.x

Jones, B., Naftz, D., Spencer, R., & Oviatt, C. 2009. Geochemical Evolution of Great Salt Lake, Utah, USA. *Aquatic Geochemistry*, *15*(1), 95–121. https://doi.org/10.1007/s10498-008-9047-y

Kahle, C. F. 1974. Ooids from Great Salt Lake, Utah, as an analogue for the genesis and diagenesis of ooids in marine limestones. *Journal of Sedimentary Petrology*, *44*(1), 30–39.

Mcdonald, D., Price, M., Goodrich, J., Nawrocki, E., Desantis, T., Probst, A., … Hugenholtz, P. 2012. An improved Greengenes taxonomy with explicit ranks for ecological and evolutionary analyses of bacteria and archaea. *The ISME Journal*, *6*(3), 610–618. https://doi.org/10.1038/ismej.2011.139

Mcgee, D., Quade, J., Lawrence Edwards, R., Broecker, W. S., Cheng, H., Reiners, P. W., & Evenson, N. 2012. Lacustrine cave carbonates: Novel archives of paleohydrologic change in the Bonneville Basin (Utah, USA). *Earth and Planetary Science Letters*, *351–352*, 182–194. https://doi.org/10.1016/j.epsl.2012.07.019

Mcguire, K. M. 2014. Comparative Sedimentology of Lake Bonneville and the Great Salt Lake, 34.

National Water Information System data available on the World Wide Web (USGS Water Data for the Nation). 2023. Retrieved from http://waterdata.usgs.gov/nwis/

O'Reilly, S. S., Mariotti, G., Winter, A. R., Newman, S. A., Matys, E. D., McDermott, F., … Klepac-Ceraj, V. 2017. Molecular biosignatures reveal common benthic microbial sources of organic matter in ooids and grapestones from Pigeon Cay, The Bahamas. *Geobiology*, *15*(1), 112–130. https://doi.org/10.1111/gbi.12196

Oviatt, C. G., Currey, D. R., & Sack, D. 1992. Radiocarbon chronology of Lake Bonneville, Eastern Great Basin, USA. *Palaeogeography, Palaeoclimatology, Palaeoecology*, *99*(3–4), 225–241. https://doi.org/10.1016/0031-0182(92)90017-Y

Oviatt, C. G., Madsen, D. B., Miller, D. M., Thompson, R. S., & McGeehin, J. P. 2015. Early Holocene Great Salt Lake, USA. *Quaternary Research*, *84*(1), 57–68. https://doi.org/10.1016/j.yqres.2015.05.001

Pacton, M., Ariztegui, D., Wacey, D., Kilburn, M. R., Rollion-Bard, C., Farah, R., & Vasconcelos, C. 2012. Going nano: A new step toward understanding the processes governing freshwater ooid formation. *Geology*, *40*(6), 547–550. https://doi.org/10.1130/G32846.1

Prevailing Wind Direction., Western Regional Climate Center, 2023. Web. 22 August 2023. http://wrcc.dri.edu/Climate/comp_table_show.php?stype=wind_dir_avg

Reitner, J. and others. 1997. *Organic matter in Great Salt Lake ooids (Utah, USA) - First approaches to a formation via organic matrices*. *Facies* (Vol. 36).

Rupke, A., & Mcdonald, A. 2012. *Great Salt Lake brine chemistry database, 1966-2011: Utah Geological Survey Open-File Report 596*. Retrieved from http://ugspub.nr.utah.gov/publications/open_file_reports/ofr-596/appa.xls

Sandberg, P. 1975. New interpretations of Great Salt Lake ooids and of ancient non-skeletal carbonate mineralogy. *Sedimentology*, *22*(4), 497–537. https://doi.org/10.1111/j.1365-3091.1975.tb00244.x

Southon, A., Santos, J. R., Druffel-Rodriguez, G. M., Southon, J., Guaciara Santos, B., Kevin Druffel-Rodriguez, B., … Maya Mazon, B. 2004. The Keck Carbon Cycle AMS Laboratory, University of California, Irvine: Initial Operation and a Background Surprise. *Radiocarbon*, *46*(46), 41–49. Retrieved from https://escholarship.org/uc/item/4522n2x6

Spencer, R.J., Eugster, H.P., and Jones, B.F. 1985. Geochemistry of Great Salt Lake, Utah II: Pleistocene-Holocene Evolution. *Geochemica et Cosmicha Acta*, *49(3)*, 739-747. https://doi.org/10.1016/0016-7037(85)90168-1.

Stephens, D. W. 1990. Changes in lake levels, salinity and the biological community of Great Salt Lake (Utah, USA), 1847-1987. *Hydrobiologia*, *197*(1), 139–146. https://doi.org/10.1007/BF00026946

Stuiver, M., & Polach, H. A. 1977. Discussion: reporting of 14 C data. *Radiocarbon*, *19*(3), 355–363. https://doi.org/10.1021/ac100494m

Stuiver, M., & Reimer, P. J. 1993. Extended ^{14}C data base and revised CALIB 3.0 ^{14}C age calibration program. *Radiocarbon*, *35*(1), 215–230.

Summons, R. E., Bird, L. R., Gillespie, A. L., Pruss, S. B., Roberts, M., & Sessions, A. L. 2013. Lipid biomarkers in ooids from different locations and ages: Evidence for a common bacterial flora. *Geobiology*, *11*(5), 420–436. https://doi.org/10.1111/gbi.12047

Talbot, M. R. 1990. A review of the palaeohydrological interpretation of carbon and oxygen isotopic ratios in primary lacustrine carbonates. Chemical Geology: Isotope Geoscience Section, 80(4), 261–279. https://doi.org/10.1016/0168-9622(90)90009-2

Trower, E. J., Lamb, M. P., & Fischer, W. W. 2017. Experimental evidence that ooid size reflects a dynamic equilibrium between rapid precipitation and abrasion rates. *Earth and Planetary Science Letters*, *468*, 112–118. https://doi.org/10.1016/j.epsl.2017.04.004

Trower, E. J., Bridgers, S. L., Lamb, M. P., & Fischer, W. W. 2020. Ooid cortical stratigraphy reveals common histories of individual co-occurring sedimentary grains. Journal of Geophysical Research: Earth Surface, 125, e2019JF005452. https://doi.org/10.1029/2019JF005452

Xu, X., Trumbore, S. E., Zheng, S., Southon, J. R., McDuffee, K. E., Luttgen, M., & Liu, J. C. 2007. Modifying a sealed tube zinc reduction method for preparation of AMS graphite targets: Reducing background and attaining high precision. *Nuclear Instruments and Methods in Physics Research Section B: Beam Interactions with Materials and Atoms*, *259*(1), 320–329. https://doi.org/10.1016/J.NIMB.2007.01.175

SUPPLEMENTARY INFORMATION

.

Methods for bulk organic and inorganic carbon extractions on sieved ooids

To obtain bulk inorganic carbon ages on sieved and unsieved ooids, ooids were dissolved in 3 extractions, and the results of those extractions were weighted and reported herein. The first CO_2 extraction occurred after 0.8 ml H_2PO_4 acid was added at 70°C and left to react for 1-2 hours. The second CO_2 extraction occurred after an additional 0.8 ml H_2PO_4 was added and left to react for 2 more hours at 70°C. The third CO_2 extraction occurred after 2 hours at 70°C after the second extraction, but no extra acid was added to the samples. All purified CO_2 samples were graphitized using a sealed-tube zinc reduction method (Xu and others, 2007). Graphite was pressed into aluminum target holders and analyzed for ^{14}C at the Keck Carbon Cycle Accelerator Mass Spectrometer (KCCAMS) facility at the University of California, Irvine (Southon and others, 2004; Beverly and others, 2010). Data were normalized and background corrected using both modern coral and radiocarbon-dead reference carbonates acidified in the same reaction vessel. Resulting fractions of modern (FM) carbon were weighted according to yield to calculate bulk inorganic carbon age, and ^{14}C data are presented according to the conventions presented in Stuiver and Polach (1977).

To measure bulk organic carbon content and radiocarbon age from the acid insoluble fraction, 1M HCl was added to 10g of ooids at 70°C for 24 hours until pH maintained at 1 for 2 hours. During acidification, the solution containing the sample was centrifuged and the solution was decanted, then a new aliquot of 1M HCl was added. This process was repeated until the pH maintained at 1 for 2 hours. The residuals were then rinsed with Milli-Q until the pH became neutral.

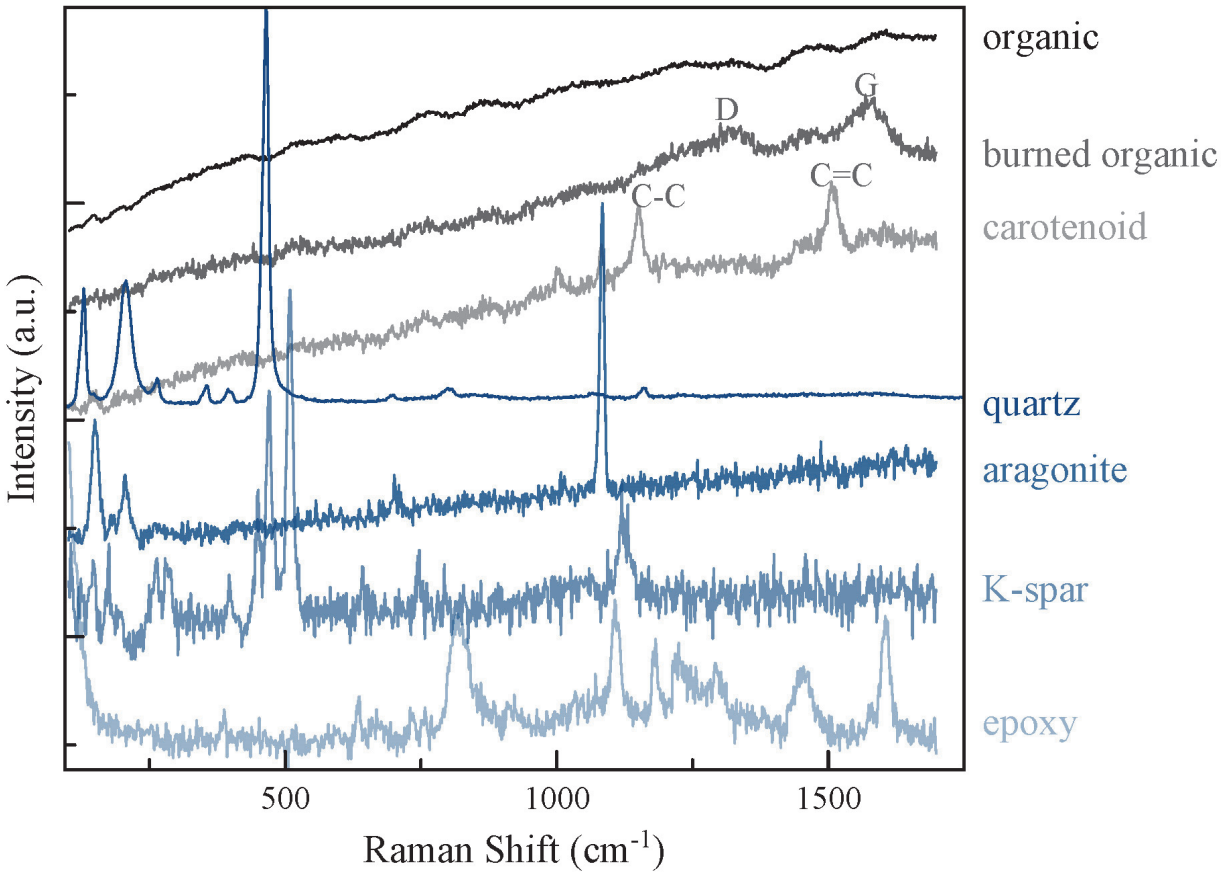

Figure 1. *Example of spectra obtained from Raman spectroscopy on one ooid demonstrating the materials identified.*

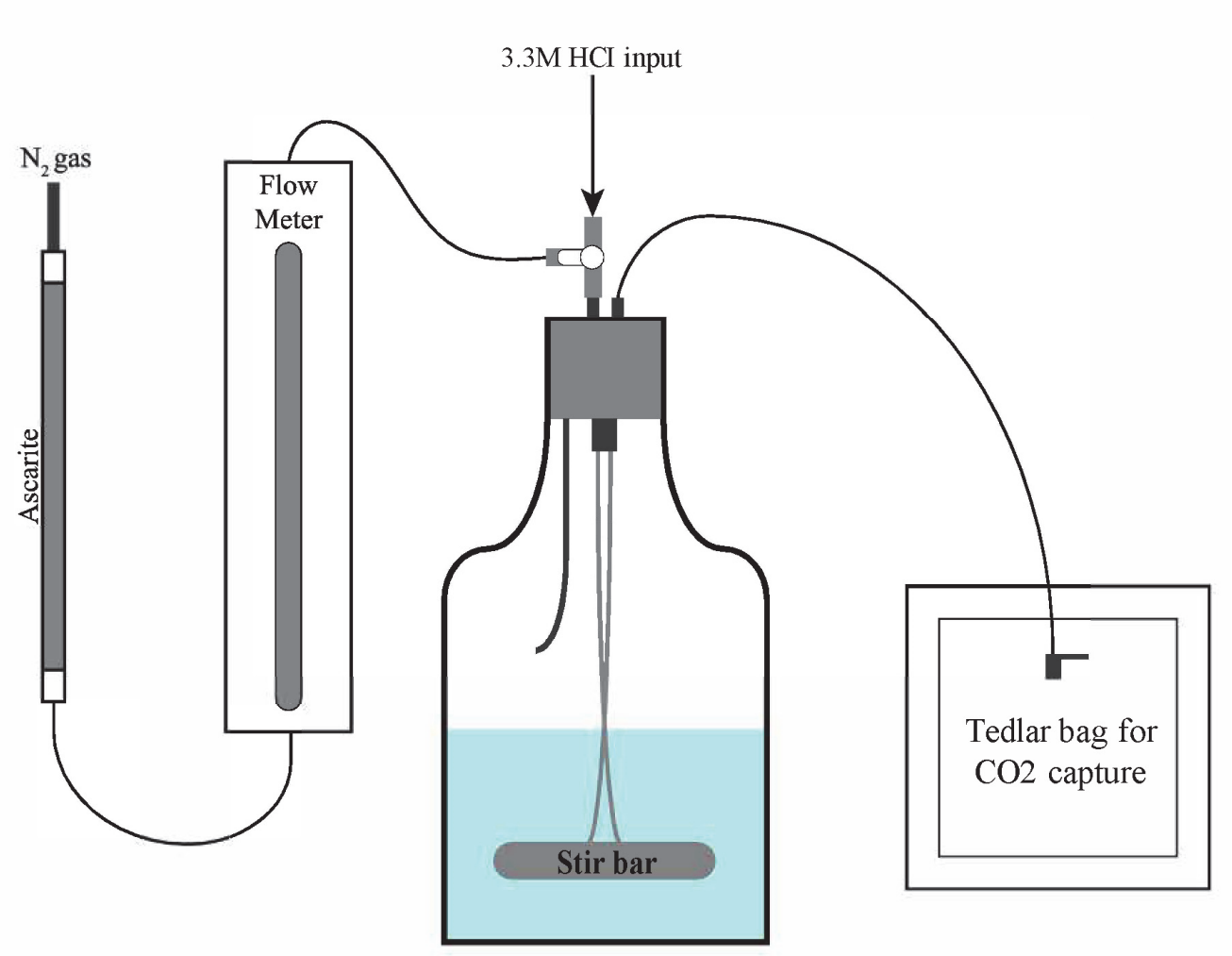

Figure 2. *Ooid dissolution reaction vessel. 50g of size-sieved ooids were added to the reaction vessel with 150cc of deionized water. Ascarite-scrubbed N2 flowed through while the stir bar spun at 600 rpm for 30 min. This step ensured no atmospheric carbon remains in the reaction vessel or water. Next, the outflow and gas inflow stopcocks were closed. For each dissolution step, 60cc of 3.3M HCl were added to the reaction vessel at a rate of 10cc/min. Tedlar bags were filled with the resulting gas every ~3min. The gas was then moved into He-rinsed and evacuated 25cc serum vials that were submitted to UC Irvine for radiocarbon analysis.*

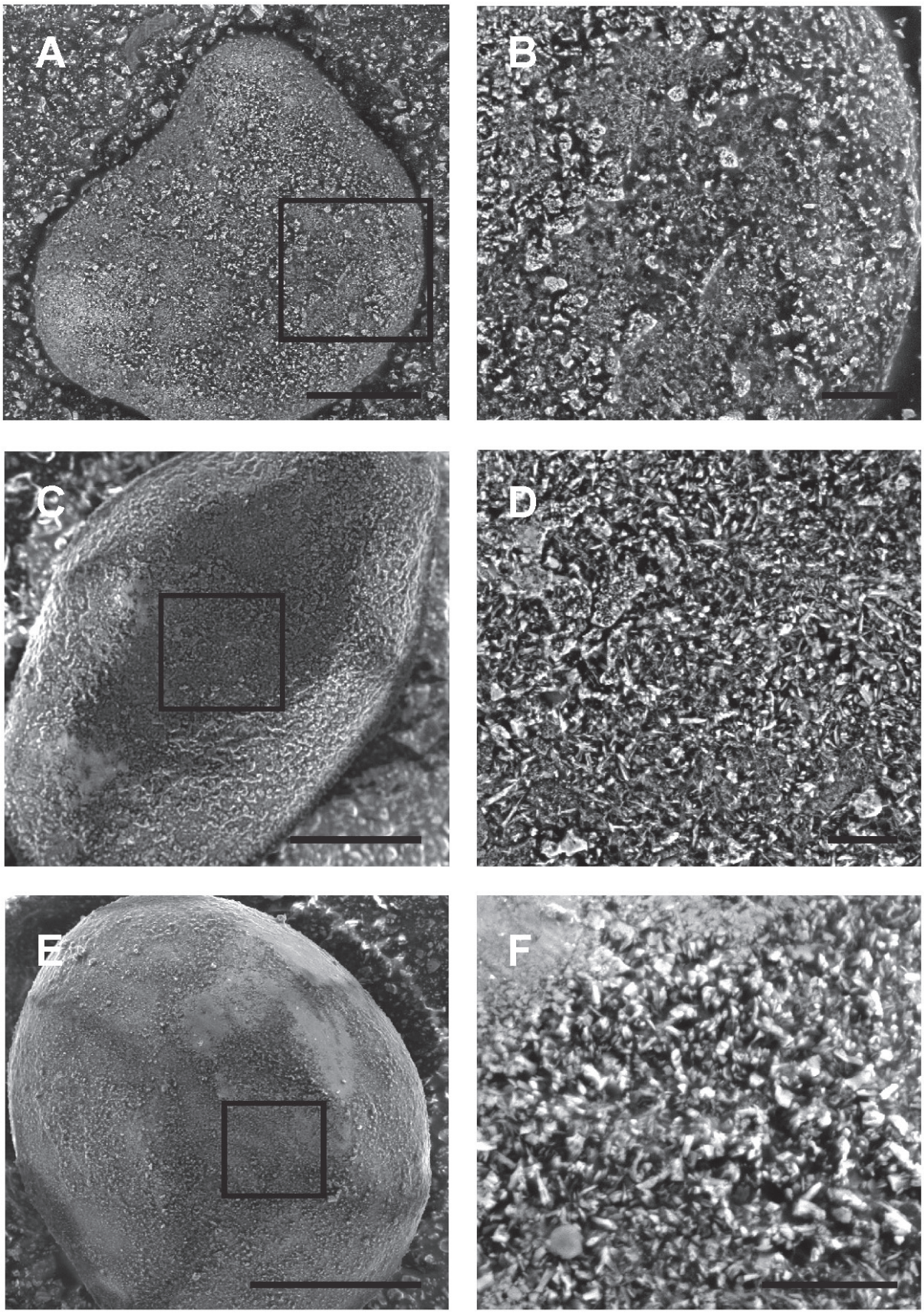

Figure 3. *Scanning electron microscope images of individual ooids with close-up inset after 60ml (A – B), 120ml (C – D), and 180ml (E – F) of 3.3M HCl was added to reaction vessel. Ooids maintain general shape post-acidification confirming dissolution occurred fairly uniformly from exterior to interior.*

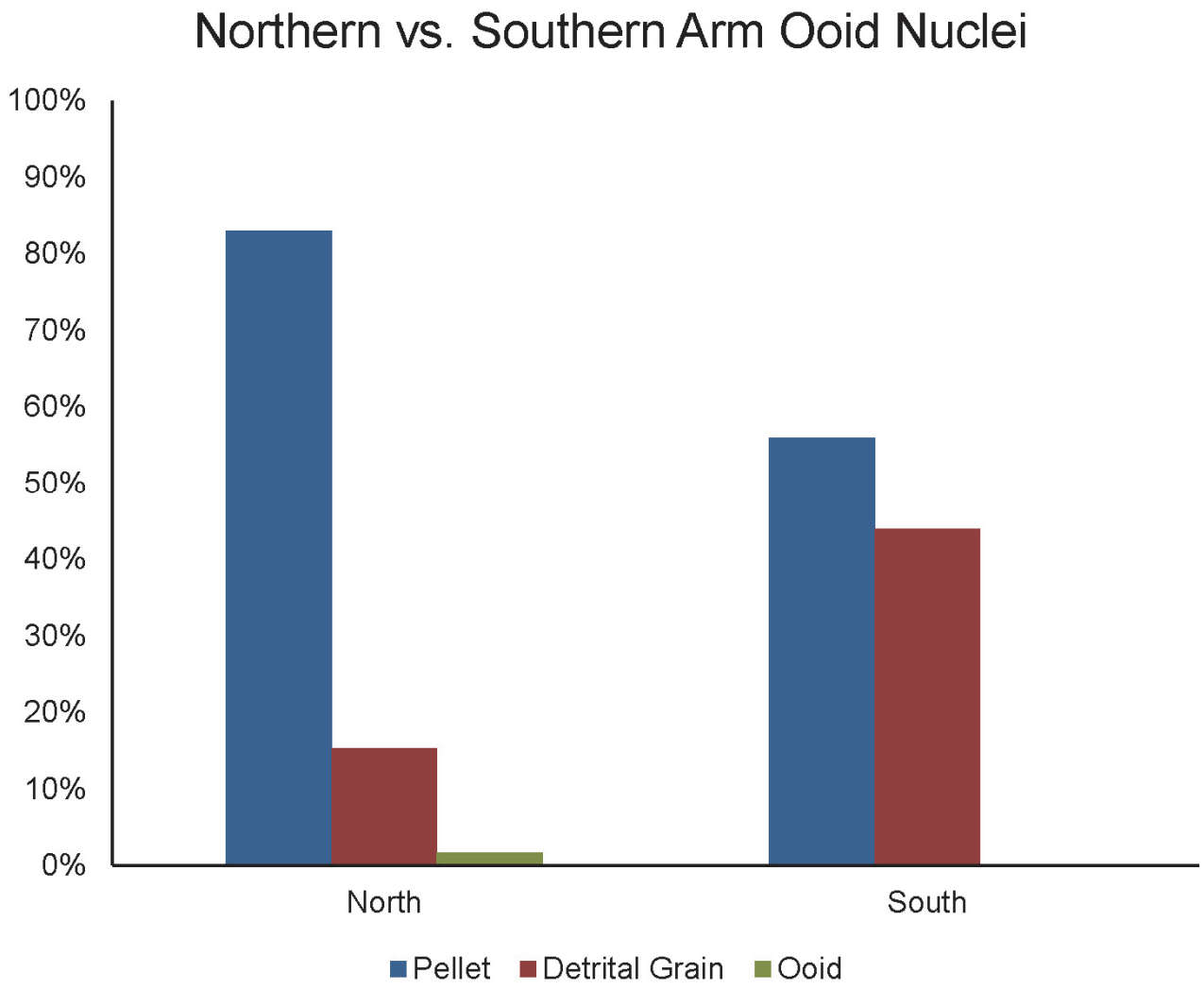

Figure 4. *Nuclei composition in north vs south arm GSL ooids as observed in thin section. North arm ooids have 83% brine shrimp pellet nuclei, 15% detrital grains such as quartz and feldspar, and 2% other ooids as nuclei. Southern arm ooids have 56% brine shrimp pellet nuclei and 44% detrital grain nuclei.*

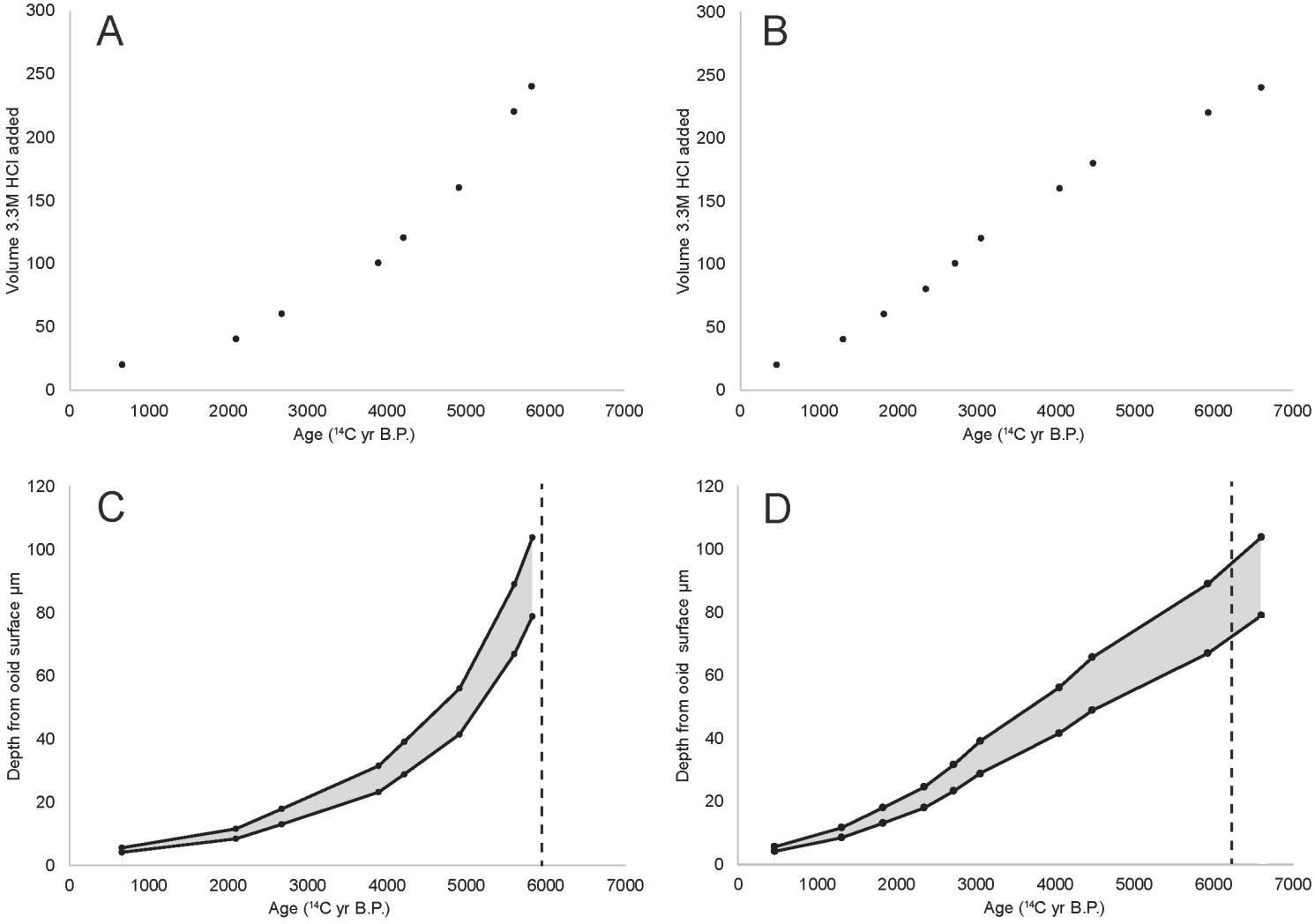

Figure 5. *Comparison of ooid chronologies from the northern arm of GSL (7B, 7D) to the southern arm of GSL (7A, 7C). Figures 7A and 7B use the radiocarbon chronology and integrate the ages assuming spherical geometry of ooids (using mean ooid radius of 213 µm). The resulting slope of the north arm ooid growth curve (B) is steeper (more rapid growth) during the first several thousand years of ooid growth and slows down during the last several thousand years, while the southern arm ooid growth curve (A) is more linear. Because north arm ooids have a larger occurrence of ooids with peloidal nuclei (roughly cylindrical geometry), the radiocarbon chronology was also integrated over an assumed cylindrical geometry using* $V = L * \pi r^2$*, where V is volume, L is length (6 * radius), and r is radius (213 µm) in micrometers. The slope of the north arm ooid growth curve remains highly non-linear even after assuming cylindrical geometry, suggesting there are other factors (environmental or otherwise) accounting for the difference in slope. The error bars represent the relations for ooids at 355 and 500 µm.*

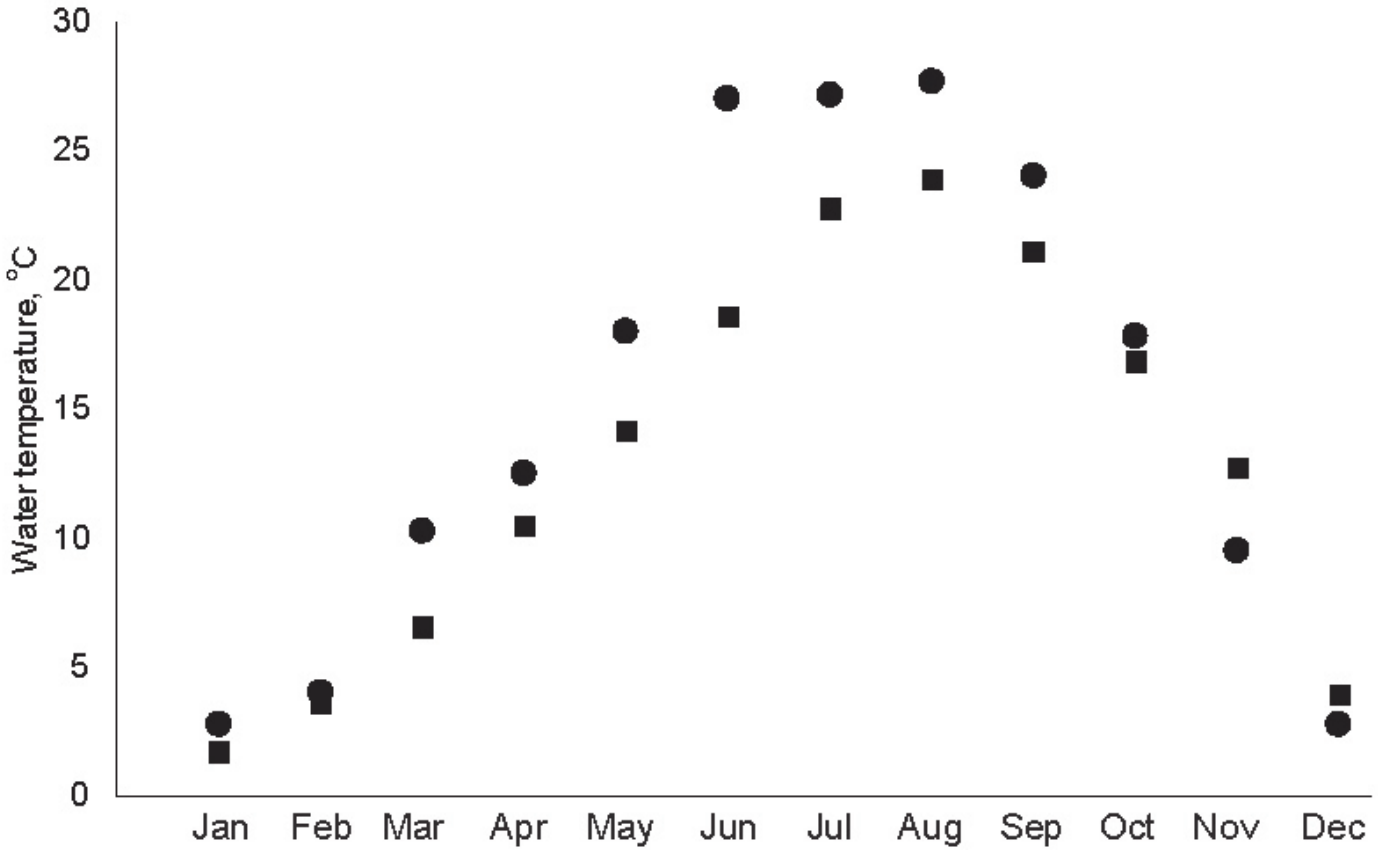

Figure 6. *Monthly average water temperature in north (circle) and south (square) arms of Great Salt Lake as measured by USGS from 2010-2016. (U.S. Geological Survey, 2016).*

Table 1. *Bulk inorganic carbon extractions for sieved and unsorted ooids. The ^{14}C ages from each extraction were pooled to calculate a bulk age for each sample.*

Grain Size (µm)	Extraction	Yield (mgC, Inorg)	Inorg C Fraction	F_m	Bulk F_m	Bulk ^{14}C Age (yr BP)
Unsorted	1	2.29	0.6844	0.7097 ± 0.0012	0.6423 ± 0.0012	3556 ± 15
	2	0.97	0.2904	0.4952 ± 0.0010		
	3	0.08	0.0252	0.5086 ± 0.0021		
355-500	1	2.36	0.6706	0.6676 ± 0.0012	0.6118 ± 0.0011	3947 ± 15
	2	0.98	0.2792	0.4977 ± 0.0009		
	3	0.18	0.0501	0.5004 ± 0.0011		
250-355	1	2.22	0.6584	0.6838 ±0.0012	0.6204 ± 0.0011	3834 ± 15
	2	1.04	0.3092	0.5024 ± 0.0009		
	3	0.11	0.0324	0.4599 ± 0.0018		
125-250	1	2.42	0.7559	0.7222 ± 0.0013	0.6749 ± 0.0012	3158 ± 15
	2	0.72	0.2257	0.5254 ± 0.0009		
	3	0.06	0.0184	0.5659 ± 0.0027		
Unsorted	1	3.29	0.7682	0.6482 ± 0.0011	0.6175 ± 0.0011	3872 ± 15
	2	0.84	0.1965	0.5202 ± 0.0010		
	3	0.15	0.0354	0.4924 ± 0.0015		
355-500	1	2.99	0.7542	0.6030 ± 0.0011	0.5802 ± 0.0011	4373 ± 20
	2	0.82	0.2055	0.5217 ± 0.0010		
	3	0.16	0.0403	0.5020 ± 0.0012		
250-355	1	2.89	0.8339	0.6491 ± 0.0011	0.6263 ± 0.0011	3759 ± 15
	2	0.52	0.1503	0.5133 ± 0.0011		
	3	0.05	0.0158	0.5010 ± 0.0031		
125-250	1	3.00	0.8602	0.7359 ± 0.0013	0.7120 ± 0.0013	2728 ± 15
	2	0.44	0.1253	0.5646 ± 0.0011		
	3	0.05	0.0145	0.5685 ± 0.0032		

Table 2. *Thin sections of individual ooids (A) analyzed with Raman spectroscopy (B) to map the presence of organic matter (blue) within the ooid cortex. A Raman spectrum with a strong noise signal suggesting the presence of organic material was selected from a GSL ooid and established as the "organic material reference spectrum". Each point on the thin section was analyzed using Raman spectroscopy and compared to the reference spectrum. The similarity of the measured spectra to the reference organic matter spectrum was mapped on thin sections with a blue overlay, with blue indicating presence of organic material.*

p.	Thin Section Label	Site	Grain Size (µm)	Ooid Number
1	AI-oc	Antelope Island – S. Arm	355 – 500	1
2	AI-oc	Antelope Island – S. Arm	355 – 500	2
3	AI-oc	Antelope Island – S. Arm	355 – 500	3
4	AI-oc	Antelope Island – S. Arm	355 – 500	4
5	AI-oc	Antelope Island – S. Arm	355 – 500	5
6	AI-om	Antelope Island – S. Arm	250 – 355	1
7	AI-om	Antelope Island – S. Arm	250 – 355	2
8	AI-om	Antelope Island – S. Arm	250 – 355	3
9	AI-om	Antelope Island – S. Arm	250 – 355	4
10	AI-om	Antelope Island – S. Arm	250 – 355	5
11	AI-of	Antelope Island – S. Arm	125 – 250	1
12	AI-of	Antelope Island – S. Arm	125 – 250	2
13	AI-of	Antelope Island – S. Arm	125 – 250	3
14	AI-of	Antelope Island – S. Arm	125 – 250	4
15	AI-of	Antelope Island – S. Arm	125 – 250	5
16	SJ-oc	Spiral Jetty – N. Arm	355 – 500	1
17	SJ-oc	Spiral Jetty – N. Arm	355 – 500	2
18	SJ-oc	Spiral Jetty – N. Arm	355 – 500	3
19	SJ-oc	Spiral Jetty – N. Arm	355 – 500	4
20	SJ-oc	Spiral Jetty – N. Arm	355 – 500	5
21	SJ-om	Spiral Jetty – N. Arm	250 – 355	1
22	SJ-om	Spiral Jetty – N. Arm	250 – 355	2
23	SJ-om	Spiral Jetty – N. Arm	250 – 355	3
24	SJ-om	Spiral Jetty – N. Arm	250 – 355	4
25	SJ-om	Spiral Jetty – N. Arm	250 – 355	5
26	SJ-of	Spiral Jetty – N. Arm	125 – 250	1
27	SJ-of	Spiral Jetty – N. Arm	125 – 250	2
28	SJ-of	Spiral Jetty – N. Arm	125 – 250	3
29	SJ-of	Spiral Jetty – N. Arm	125 – 250	4